Bose-Einstein condensation of trapped interacting spin-1 atoms

Wenxian Zhang,[1] Su Yi,[2] and L. You[1]

[1]*School of Physics, Georgia Institute of Technology, Atlanta, Georgia 30332-0430, USA*
[2]*Department of Physics and Astronomy and Rice Quantum Institute,*
Rice University, Houston, Texas 77251-1892, USA
(Dated: 14 June 2004)

We investigate Bose-Einstein condensation of trapped spin-1 atoms with ferromagnetic or antiferromagnetic two-body contact interactions. We adopt the mean field theory and develop a Hartree-Fock-Popov type approximation in terms of a semiclassical two-fluid model. For antiferromagnetic interactions, our study reveals double condensations as atoms in the $|m_F = 0\rangle$ state never seem to condense under the constraints of both the conservation of total atom number N and magnetization M. For ferromagnetic interactions, however, triple condensations can occur. Our results can be conveniently understood in terms of the interplay of three factors: (anti) ferromagnetic atom-atom interactions, M conservation, and the miscibilities between and among different condensed components.

I. INTRODUCTION

Research in dilute atomic quantum gases remains one of the most vibrant areas in physics almost ten years after the landmark discovery of atomic Bose-Einstein condensation (BEC). Increasingly, new experiments are revealing the rich possibilities afforded by the internal electronic state structures of an atom, e.g., the generation of atom entanglement in the Mott phase through controlled collisions from the relative displacement of the optical lattice potentials of the respective atomic internal states [1] and the recent observation of condensation of fermionic atom pairs [2].

It has been known for a long time that the spinor degrees of freedom of an atom becomes accessible if a far-off-resonant optical trap is used to provide equal confinement for all Zeeman states, instead of the more widely used magnetic traps for spin polarized atoms [3, 4, 5, 6]. Several earlier experiments have produced fascinating observations of spinor condensates, a superfluid with internal degrees of freedom, e.g., with ^{23}Na atoms in $F = 1$ [7] and $F = 2$ [8] and ^{87}Rb atoms in $F = 1$ [9, 10] and $F = 2$ [11, 12], spin domains and interdomain tunnelling [13, 14], as well as the generation of coreless vortex states [15, 16, 17, 18]. These properties exist only because of the spinor nature of the condensate order parameter, and thus are generally not expected to occur in a magnetically trapped condensate.

Despite these and other related successes with spinor condensates, our knowledge remains limited regarding the condensation thermodynamics of spin-1 atoms. In a sense, the spin-1 condensate constitutes a type of quantum fluid unfamiliar to many of us. On the experimental side, it remains a significant challenge to produce a spinor condensate, as evidenced by the disproportionally small numbers of spinor BEC experiments in operation. In this article, we reconsider the topic of the condensation thermodynamics for a system of trapped spin-1 atoms. Of

particular interest to us is the question of the so-called double condensations for a spin-1 system constrained by two global conservations [19]. Using the Bogoliubov-Popov approximation, Isoshima *et al.* first investigated the thermodynamics of the BEC phase transition for a spin-1 gas [19]. Huang *et al.* studied analytically the effect of a magnetic field on the transition temperature [20]. While an attempt to find the zero-magnetic-field phase diagram was made through numerical simulations in Ref. [19], there still exist several question marks to the overall picture of BEC for a spin-1 Bose gas, especially for ferromagnetically interacting atoms such as ^{87}Rb. Limited by the computation procedure within the Bogoliubov-Popov approximation, only a few data points were made available in the earlier studies by Isoshima *et al.* [19]. The lack of focused experimental efforts also indirectly discouraged a detailed investigation of this problem until now.

In this paper we systematically investigate the phase diagram of a spin-1 Bose gas for both ferromagnetic and antiferromagnetic interactions. Instead of the Bogoliubov approach, we will adopt the Hartree-Fock-Popov approximation and employ a semiclassical approximation to the noncondensed atoms within the mean field theory. We will also enforce the thermodynamics for a finite trapped system with a fixed total atom number N and a total magnetization M. Recent studies have significantly verified the accuracy of this approximation when applied to similar systems [21]. As we will illustrate in this work our results indicate that double condensations will occur for a spin-1 gas with antiferromagnetic interactions, while triple condensations are more likely for ferromagnetic interactions.

This paper is organized as follows. In Sec. II, we review the additional features of a BEC for an ideal gas of spin-1 atoms. This is followed by the discussion of an interacting spin-1 gas in Sec. III and a brief sketch of the Hartree-Fock-Popov theory used for our investiga-

tion. We outline the detailed numerical algorithm used to solve the coupled two-fluid model quantum gas at different temperatures in Sec. IV and present the results of our study in Sec. V. We conclude with some discussions and remarks in Sec. VI.

II. BEC OF AN IDEAL GAS OF SPIN-1 ATOMS

In this section, we briefly review the phenomenon of a BEC for a trapped noninteracting gas of spin-1 atoms following the pioneering study of Isoshima et $al.$ [19]. At thermal equilibrium, we adopt the standard Bose-Einstein distribution, and treat the spinor degree of freedom as degenerate internal states in the absence of an external magnetic field. The average number of atoms at each single atom state of an energy ε_j for the component $|F = 1, m_F = i\rangle$, $i = +1, 0$, and -1 (hereafter $|i\rangle$), is then conveniently given by

$$N_{i,j} = \frac{z_i e^{-\beta \varepsilon_j}}{1 - z_i e^{-\beta \varepsilon_j}}, \tag{1}$$

with $\beta = 1/(k_B T)$ at temperature T. k_B is the Boltzmann constant. The fugacity z_i can be expressed in terms of the chemical potential for the ith component μ_i as $z_i = \exp(\beta \mu_i)$. In the thermodynamic limit, one can follow the usual approach by making a semiclassical approximation for a continuous description of the single particle density of states, and treating the ground state population separately as it can become macroscopic due to Bose-Einstein condensation. The total number of atoms for a given internal state in all motional excited states of the trap is thus found to be

$$N_i^T = \sum_{j=1}^{\infty} N_{i,j} = \left(\frac{k_B T}{\hbar \omega}\right)^3 g_3(z_i), \tag{2}$$

where we have assumed atoms are confined in a spherical harmonic trap with a frequency ω independent of the atomic internal state $|i\rangle$. $g_\xi(x) = \sum_{n=1}^{\infty}(x^n/n^\xi)$ is the standard Bose function [22, 23]. We note that the conservations of the total number of atoms $N = N_+ + N_0 + N_-$ and total magnetization $M = N_+ - N_-$ lead to the chemical potentials for different spin components expressible as $\mu_\pm = \mu \pm \eta$ and $\mu_0 = \mu$. These identities remain valid in the presence of atom-atom interactions. μ and η are effectively independent Lagrange multipliers used to guarantee the conservation of N and M, respectively. Taking the single atom trapped ground state to be zero energy, the Bose distribution (1) shows that μ_i is negative at high temperatures and reaches zero when the spin component $|i\rangle$ condenses. η is positive (negative) for a positive M (negative), which acts as a fictitious applied magnetic field physically.

As was first pointed out in Ref. [19], there exists an interesting double condensation phenomenon for a spin-1 gas because of the presence of M conservation. When the temperature is lowered, the $|+\rangle$ component first condenses for a system with a positive M because its phase space density is largest, reflecting the fact that N_+ is the largest component population. Thus we first arrive at $\mu_+ = 0$. This consideration leads to the critical temperature T_1 governed by the following equations:

$$N = \left(\frac{k_B T_1}{\hbar \omega}\right)^3 \left[g_3(1) + g_3(e^{\beta \mu}) + g_3(e^{2\beta \mu})\right], \tag{3}$$

$$M = \left(\frac{k_B T_1}{\hbar \omega}\right)^3 \left[g_3(1) - g_3(e^{2\beta \mu})\right]. \tag{4}$$

On further lowering of the temperature, however, the remaining two components $|0\rangle$ and $|-\rangle$ condense simultaneously, rather than sequentially with the less populated component of the two condensing last. This is precisely due to the conservation identities as discussed before. The relationships $\mu_\pm = \mu \pm \eta$ and $\mu_0 = \mu$ lead to a mathematical certainty: when μ_+ is zero, if either μ_0 or μ_- becomes zero, both must be zero. At this second critical temperature T_2, both $\mu_0 = 0$ and $\mu_- = 0$, which imply that the $|0\rangle$ and $|-\rangle$ components condense simultaneously. This second condensation where all three components condense, occurs at the temperature T_2 of

$$T_2 = \frac{\hbar \omega}{k_B} \left[\frac{N - M}{3 g_3(1)}\right]^{1/3}. \tag{5}$$

In Fig. 1, we illustrate the M dependence of the double condensations for an ideal Bose gas of spin-1 atoms. $T_c = [N/g_3(1)]^{1/3}(\hbar\omega/k_B) \approx 0.94 N^{1/3}\hbar\omega/k_B$ is the condensation temperature for $M = N$, i.e., for a single component gas with all atoms polarized in state $|+\rangle$.

III. BEC OF AN INTERACTING GAS OF SPIN-1 ATOMS

A. Formulation

Our model system of the interacting spin-1 atoms is described by the following Hamiltonian in second quantized form

$$H = \int d\vec{r} \left\{ \psi_i^\dagger \left[-\frac{\hbar^2}{2m}\nabla^2 + V_{\text{ext}}(\vec{r})\right] \psi_i + \frac{c_0}{2} \psi_i^\dagger \psi_j^\dagger \psi_j \psi_i \right.$$
$$\left. + \frac{c_2}{2} \psi_i^\dagger (F_\alpha)_{ij} \psi_j \psi_k^\dagger (F_\alpha)_{kl} \psi_l \right\}, \tag{6}$$

where $\psi_i(\vec{r})$ $[\psi_i^\dagger(\vec{r})]$ is the quantum field for annihilating an atom in state $|i\rangle$ at $\vec{r}$, and $i, j, k, l = +, 0, -$ and $\alpha = x, y, z$. Repeated indices are assumed to be summed [3, 4]. $F_{\alpha=x,y,z}$ are spin-1 matrices given by

$$F_x = \frac{1}{\sqrt{2}} \begin{pmatrix} 0 & 1 & 0 \\ 1 & 0 & 1 \\ 0 & 1 & 0 \end{pmatrix},$$
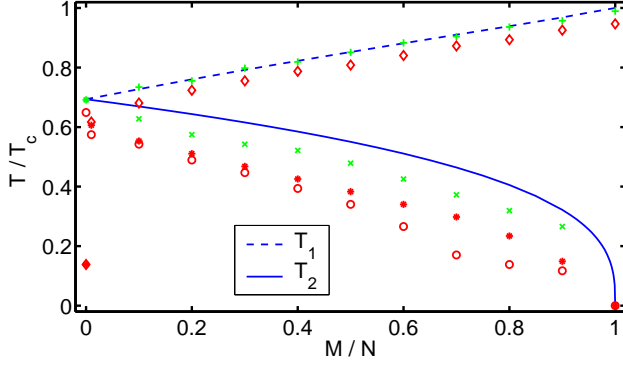
FIG. 1: BEC for a gas of spin-1 atoms with $M > 0$ ($M < 0$). For noninteracting atoms, the $|+\rangle$ ($|-\rangle$) component condenses first at T_1 (dashed line) while the $|0\rangle$ and $|-\rangle$ ($|+\rangle$) components condense simultaneously at T_2 (solid line). For ^{23}Na atoms with antiferromagnetic interactions, double condensations persist according to our theoretical study. The $|+\rangle$ component (denoted by $+$) condenses first, which is then followed by the condensation of the $|-\rangle$ component (denoted by $\times$). The $|0\rangle$ component is unpopulated in the low temperature limit. For ^{87}Rb atoms with ferromagnetic interactions, our study reveals the potential for triple condensations. First, the $|+\rangle$ component condenses (denoted by $\diamond$), which is then followed by the second condensation for the $|-\rangle$ component (denoted by $*$), and finally the third condensation for the $|0\rangle$ component occurs (denoted by $\circ$).

$$F_y = \frac{i}{\sqrt{2}} \begin{pmatrix} 0 & -1 & 0 \\ 1 & 0 & -1 \\ 0 & 1 & 0 \end{pmatrix},$$

$$F_z = \begin{pmatrix} 1 & 0 & 0 \\ 0 & 0 & 0 \\ 0 & 0 & -1 \end{pmatrix},$$

with the quantization axis taken along the z-axis direction. It is easy to check that both the total number of atoms and the total magnetization

$$N = \int d\vec{r}(|\psi_+|^2 + |\psi_0|^2 + |\psi_-|^2),$$

$$M = \int d\vec{r}(|\psi_+|^2 - |\psi_-|^2) = \int d\vec{r}\psi_i^\dagger (F_z)_{ij}\psi_j,$$

commute with the above Hamiltonian (6), and are thus constants of motion. To study the minimal energy ground state, we therefore introduce two Lagrange multipliers μ and η, to fix the total atom number and magnetization of the system in our numerical minimization. It turns out that μ is in fact the chemical potential of the system and η is an effective magnetic field. The Gibbs free energy is then given by

$$\begin{aligned} G &= H - \mu N - \eta M \\ &= \int d\vec{r} \Big\{ \psi_i^\dagger (\mathcal{L}_{ij} - \eta(F_z)_{ij})\psi_j + \frac{c_0}{2}\psi_i^\dagger \psi_j^\dagger \psi_j \psi_i \\ &\quad + \frac{c_2}{2} \psi_i^\dagger (F_\alpha)_{ij} \psi_j \psi_k^\dagger (F_\alpha)_{kl} \psi_l \Big\}, \end{aligned} \tag{7}$$

where

$$\mathcal{L}_{ij} = \left[-\frac{\hbar^2}{2m}\nabla^2 - \mu + V_{\text{ext}}(\vec{r}) \right] \delta_{ij}.$$

The atomic interactions are conveniently parametrized through the two s-wave scattering lengths a_0 and a_2 between two spin-1 atoms [3, 4, 5]

$$c_0 = \frac{4\pi\hbar^2}{m} \left(\frac{a_0 + 2a_2}{3} \right),$$

$$c_2 = \frac{4\pi\hbar^2}{m} \left(\frac{a_2 - a_0}{3} \right).$$

In this study, we attempt to find the mean field ground state of our system, which corresponds to the state with the lowest Gibbs free energy.

B. Hartree-Fock-Popov theory and the two-fluid model approximations

The field operator $\psi(\vec{r}, t)$ evolves in the Heisenberg picture according to

$$i\hbar\frac{\partial}{\partial t}\psi(\vec{r}, t) = [\psi, G].$$

For the system of a spin-1 Bose gas as considered here, the above equation becomes

$$i\hbar\frac{\partial}{\partial t}\psi_+(\vec{r}, t) = \mathcal{L}_{++}\psi_+ - \eta\psi_+ + c_0 \sum_j \left(\psi_j^\dagger \psi_j \right) \psi_+ + c_2 \left[\left(\psi_+^\dagger \psi_+ + \psi_0^\dagger \psi_0 - \psi_-^\dagger \psi_- \right) \psi_+ + \psi_-^\dagger \psi_0 \psi_0 \right],$$

$$i\hbar\frac{\partial}{\partial t}\psi_0(\vec{r}, t) = \mathcal{L}_{00}\psi_0 + c_0 \sum_j \left(\psi_j^\dagger \psi_j \right) \psi_0 + c_2 \left[\left(\psi_+^\dagger \psi_+ + \psi_-^\dagger \psi_- \right) \psi_0 + 2\psi_0^\dagger \psi_+ \psi_- \right], \tag{8}$$

$$i\hbar\frac{\partial}{\partial t}\psi_-(\vec{r}, t) = \mathcal{L}_{--}\psi_- + \eta\psi_- + c_0 \sum_j \left(\psi_j^\dagger \psi_j \right) \psi_- + c_2 \left[\left(\psi_-^\dagger \psi_- + \psi_0^\dagger \psi_0 - \psi_+^\dagger \psi_+ \right) \psi_- + \psi_+^\dagger \psi_0 \psi_0 \right].$$

Following the standard mean field theory procedure, i.e. taking $\psi = \phi + \delta\psi$ with $\phi = \langle\psi\rangle$, after tedious manipulations and calculations, we obtain a set of coupled Gross-Pitaevskii equations for the superfluid components including their

interactions with the noncondensed atoms as

$$i\hbar\frac{\partial}{\partial t}\phi_+ = \left[-\frac{\hbar^2}{2m}\nabla^2 + V_{\text{ext}} - \mu - \eta + c_0(n + n_+^T) + c_2(n_+ + n_0 - n_- + n_+^T)\right]\phi_+ + c_2\phi_0^2\phi_-^*,$$

$$i\hbar\frac{\partial}{\partial t}\phi_0 = \left[-\frac{\hbar^2}{2m}\nabla^2 + V_{\text{ext}} - \mu + c_0(n + n_0^T) + c_2(n_+ + n_-)\right]\phi_0 + 2c_2\phi_+\phi_-\phi_0^*, \tag{9}$$

$$i\hbar\frac{\partial}{\partial t}\phi_- = \left[-\frac{\hbar^2}{2m}\nabla^2 + V_{\text{ext}} - \mu + \eta + c_0(n + n_-^T) + c_2(n_- + n_0 - n_+ + n_-^T)\right]\phi_- + c_2\phi_0^2\phi_+^*,$$

and equations for $\delta\psi_i$,

$$i\hbar\frac{\partial}{\partial t}\delta\psi_+(\vec{r}, t) = \left[-\frac{\hbar^2}{2m}\nabla^2 + V_{\text{ext}} - \mu - \eta + c_0(n + n_+) + c_2(2n_+ + n_0 - n_-)\right]\delta\psi_+,$$

$$i\hbar\frac{\partial}{\partial t}\delta\psi_0(\vec{r}, t) = \left[-\frac{\hbar^2}{2m}\nabla^2 + V_{\text{ext}} - \mu + c_0(n + n_0) + c_2(n_+ + n_-)\right]\delta\psi_0, \tag{10}$$

$$i\hbar\frac{\partial}{\partial t}\delta\psi_-(\vec{r}, t) = \left[-\frac{\hbar^2}{2m}\nabla^2 + V_{\text{ext}} - \mu + \eta + c_0(n + n_-) + c_2(2n_- + n_0 - n_+)\right]\delta\psi_-,$$

where $n = \sum_i n_i = \sum_i(|\phi_i|^2 + n_i^T)$ is the total density of the atomic gas, with $n_i^T = \langle\delta\psi_i^\dagger\delta\psi_i\rangle$ the normal (noncondensed) gas density of the ith component. Instead of the Hartree-Fock-Bogoliubov (HFB) approximation as employed by Isoshima *et al.* [19], we have used the Hartree-Fock-Popov (HFP) approximation to obtain the above equations. Within the HFP approximation, we neglect terms proportional to the anomalous noncondensate density $\langle\delta\psi_i\delta\psi_j\rangle$ as well as their complex conjugates. We have also neglected terms proportional to $\langle\delta\psi_i^\dagger\delta\psi_j\rangle$ for $i \neq j$, similar to the random phase approximation. A more detailed formal discussion of the HFP theory can be found in Refs. [24, 25], and for the calculation of the phase diagram of Bose-Einstein condensation, it is an excellent approximation as confirmed recently in a set of detailed comparisons with experiments [21]. In addition, as will become clear later, the HFP approximation is also efficient from the numerical point of view, especially near regions of temperatures close to (but below) the critical temperature. The HFB approximation, on the other hand, is more difficult to handle numerically [19]. Although more rigorous at very low temperatures, the HFB approximation is expected to agree with the more transparent HFP approximation at higher temperatures. In deriving the equations for $\delta\psi_i$, terms proportional to $\delta\psi_i^\dagger$, $\delta\psi_j$, and $\delta\psi_j^\dagger$ for $j \neq i$ are also neglected. This is equivalent to the neglect of the "hole" component in the HFB approximation, and is thus expected to have has a minor effect except very close to the zero temperature.

In the HFP approximation we adopt here, the normal fluid for noncondensed atoms is determined through the semi-classical approximation. We thus take $-i\hbar\nabla \to \vec{p}$, and approximate its distribution by the standard Bose-Einstein distribution in the phase space of $\{\vec{p}, \vec{r}\}$,

$$n_i^T(\vec{r}) = \int \frac{d\vec{p}}{(2\pi\hbar)^3} \frac{1}{e^{\varepsilon_i(\vec{p}, \vec{r})/k_B T} - 1}, \tag{11}$$

with the HFP single particle energy spectrum,

$$\varepsilon_+(\vec{p}, \vec{r}) = \frac{p^2}{2m} + V_{\text{ext}} - \mu - \eta + c_0(n + n_+)$$
$$+ c_2(2n_+ + n_0 - n_-),$$

$$\varepsilon_0(\vec{p}, \vec{r}) = \frac{p^2}{2m} + V_{\text{ext}} - \mu + c_0(n + n_0) + c_2(n_+ + n_-),$$

$$\varepsilon_-(\vec{p}, \vec{r}) = \frac{p^2}{2m} + V_{\text{ext}} - \mu + \eta + c_0(n + n_-)$$
$$+ c_2(2n_- + n_0 - n_+), \tag{12}$$

which are obtained by substituting $\delta\psi_i(\vec{r}, t) = \exp[-i\varepsilon_i(\vec{p}, \vec{r})t/\hbar]u_i(\vec{r})$ into Eqs. (10) with $u_i(\vec{r})$ the eigenfunction for the excitation of the ith component.

Thus, we have formulated a coupled set of equations for both the superfluid and the normal fluid; they are Eq. (9) for the condensed part and Eqs. (11) and (12) for the noncondensed atoms. These are the basis for our numerical investigations to be presented below.

IV. NUMERICAL METHOD

In our numerical studies, we follow a standard procedure and the following algorithm for the self-consistent solution of the coupled equations (9), (11), and (12) as an extension of the single component gas studied earlier [24]. Our algorithm is divided into the following steps:

- We find the condensate wave function $\phi_i(\vec{r})$ and the chemical potential μ for a set of fixed normal gas density $n_i^T(\vec{r})$, by propagating Eqs. (9) in the

imaginary time domain, as described in Refs. [26, 27].

- We compute the updated energy spectrum and normal gas density $n_i^T(\vec{r})$ from Eqs. (11) and (12) using the new condensate wave function and the chemical potential.

- We normalize the total number of atoms to N and adjust η appropriately [26].

- We repeat the above steps until final convergence is reached. The convergence criterion is set to be that the condensate fraction $N^C(T)/N$ and the magnetization fraction M/N of successive iterations differ by less than 10^{-11} for most temperatures and less than 10^{-5} near the phase transition temperature region.

At temperatures higher than the first BEC transition point, the above procedure converges rather quickly as the superfluid component ϕ_i is none existent. In this case, we only need to solve Eqs. (11) and (12) self-consistently by adjusting μ and η.

V. RESULTS AND DISCUSSION

In this study, we focus on the illustration of our theory for atoms inside a spherically symmetric harmonic trap

$$V_{\text{ext}}(\vec{r}) = \frac{1}{2}m\omega^2 r^2. \tag{13}$$

We take $N = 10^6$ and $\omega = (2\pi)100$ Hz, and use the spin-1 atom parameters for ^{23}Na and ^{87}Rb atoms as given in Table I. Clearly it is antiferromagnetic ($c_2 > 0$) for ^{23}Na atoms and ferromagnetic ($c_2 < 0$) for ^{87}Rb atoms.

TABLE I: Atomic parameters for ^{23}Na and ^{87}Rb atoms [28, 29]. a_0 and a_2 are in units of Bohr radius and c_0 and c_2 in units of 10^{-12} Hz cm^3.

	a_0	a_2	c_0	c_2
^{23}Na	50.0	55.0	15.587	0.4871
^{87}Rb	101.8	100.4	7.793	-0.0361

A. ^{23}Na atoms with antiferromagnetic interactions

The interaction between ^{23}Na atoms is antiferromagnetic, i.e. $c_2 > 0$. The phase diagram we obtain is shown in Fig. 2. It clearly reveals the double phase transitions: one for the $|+\rangle$ component and the other for the $|-\rangle$ component. The $|0\rangle$ component of the condensate never shows up because the antiferromagnetic interaction favors an antiparallel alignment of the atomic spin, which is equivalent to a coherent superposition of the $|+\rangle$ and $|-\rangle$ states as explained in the discussion of order parameter
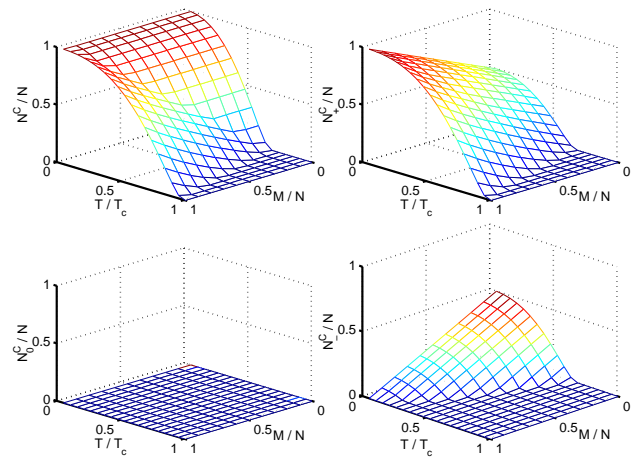

FIG. 2: Double condensations for a spin-1 gas of ^{23}Na atoms. The upper left panel shows the total condensed fraction vs temperature and total magnetization. Similarly, the upper right one shows the fraction of condensed $|+\rangle$ component, the lower left the condensed $|0\rangle$ component, and the lower right the condensed $|-\rangle$ component.

symmetry at zero temperature in Ref. [3]. Our mean field result is also consistent with that of Isoshima *et al.* [19]. Similar to the case of an ideal gas, the transition temperature of the $|+\rangle$ component increases monotonically with M/N while that of the $|-\rangle$ component monotonically decreases. When the temperature decreases, the first condensed component is $|+\rangle$ because $M > 0$; the second condensed component is $|-\rangle$, which condenses at temperatures when $N_+^C + N_+^T - N_-^T > M$. Figure 3 shows typical density distributions of different components for a ^{23}Na gas. We see that $|\phi_+|^2$ and $|\phi_-|^2$ are always miscible [30, 31] and distributed mostly near the central region of the trap. We also note that $|\phi_0|^2$ is always zero within this mean field study. All three components of the normal gas coexist. Both n_+^T and n_-^T peak at the edge of the condensate because of the shape of the net interaction potentials between the condensate and the normal gas. n_0^T is much flatter since $|\phi_0|^2$ is zero.

We now comment on a particular feature related to the asymptotic behavior of the spin-1 gas of ^{23}Na atoms as $T \to 0$ for $M = 0$. The full quantum theory predicts a ground as a superfragmented Fock state with atoms equally distributed among the three spin components $|N_+ = N/3, N_0 = N/3, N_- = N/3\rangle$ [3, 5, 32, 33]. Such a state would give rise to a number fluctuation of order of N^2, and is impossible within the present mean field treatment. The mean field ground state is known to be $|N_+ = N/2, N_0 = 0, N_- = N/2\rangle$ [32, 34], consistent with our results. In an actual experiment, it is most likely that the mean field ground state is observed because the full quantum state is not stable against various external sources of fluctuation or noises, e.g. that of the unshielded magnetic field [33], a small deviation of the total magnetization M from zero [32], or a temperature being not exactly zero. The mean field ground state, on
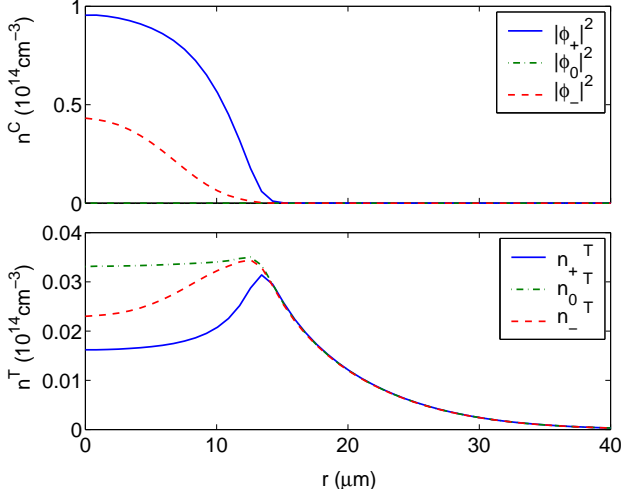
FIG. 3: Typical density distributions for different spin components of a ^{23}Na gas ($T/T_c = 0.43, M/N = 0.4$). The upper panel is for the condensate and the lower one for the noncondensed atoms.

FIG. 4: The same as in Fig. 2 but for a gas of ^{87}Rb atoms.

the other hand, is more robust against these noise. In our numerical calculations, it is really impractical to set the temperature microscopically close to but above zero to probe the real ground state (for $M = 0$). We therefore enforced the ground state structure such that it asymptotically approaches that of the mean field ground state with a decrease of the temperature as shown in Fig. 2. With this convention, an related issue arises: the equivalence between states $|N_+ = N/2, N_0 = 0, N_- = N/2\rangle$ and $|N_+ = 0, N_0 = N, N_- = 0\rangle$ at zero temperature as first pointed out by Ho [3]. We note, however, that this equivalence is based on the assumption of an environment perfectly free of magnetic fields. The presence of even a tiny magnetic field, which is inevitable in the real world, will destroy this equivalence and causing the real ground state to be $|N_+ = N/2, N_0 = 0, N_- = N/2\rangle$, a convention we chose as indicated in Fig. 2.

B. ^{87}Rb atoms with ferromagnetic interactions

The phase diagrams for ^{87}Rb atoms with ferromagnetic interactions ($c_2 < 0$) are shown in Figs. 4 and 5. Only a sparse set of points weas made available in the early work of Isoshima et $al.$ [19] because the numerical solution becomes far more difficult to converge in this case. Based on our results, we see that when the temperature of the system decreases, triple condensations occur in general. When $M > 0$, the first condensed component is the $|+\rangle$ state (for $T < T_1$), the second one is the $|-\rangle$ state (for $T < T_2$), and the last one is the $|0\rangle$ state (for $T < T_3$). Our results show that the $|+\rangle$ component first condenses at T_1 and its population increases with decreasing temperature until T_2, at which the $|+\rangle$ condensed component is a little more than the total magnetization M. When
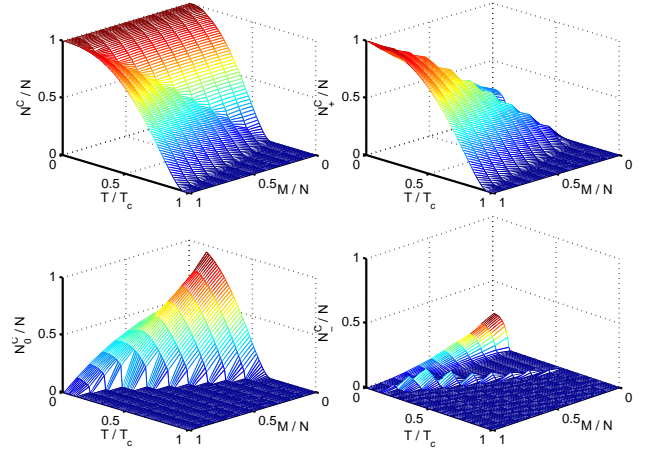
temperature is lower than T_2, the $|-\rangle$ component begins to condense as well. The two condensed components in states $|+\rangle$ and $|-\rangle$ both increase with decreasing temperature until the third critical temperature T_3, at which the $|0\rangle$ component starts to condense. Once the $|0\rangle$ component condenses, the $|-\rangle$ component starts to decrease and becomes very close to zero, while the $|+\rangle$ component is almost constant with respect to further decreasing of the temperature. This trend continues until the temperature is lower than T_4, when the condensed $|0\rangle$ component starts to decrease with decreasing temperature while the populations of the $|+\rangle$ and $|-\rangle$ condensed components increase. For the special case of $M = 0$, on the other hand, we observe only double condensations; the $|0\rangle$ component condenses first, followed by the simultaneous condensation of both the $|+\rangle$ and $|-\rangle$ components. This is again due to the special symmetry requirement that the $|+\rangle$ component must be the same as the $|-\rangle$ component in order to keep $M = 0$. We note that in this case the fraction of condensed $|0\rangle$ component can reach as high as 94% at finite temperatures, much higher than the $\sim 50\%$ at zero temperature.

Figure 6 displays typical density distributions for a gas of ^{87}Rb atoms at different temperatures for $M/N = 0.6$. The right column corresponds to $T \in (T_3, T_2]$, where only the $|+\rangle$ and $|-\rangle$ components are condensed and the $|-\rangle$ component is quite small and is spatially located at the edge of the $|+\rangle$ component. Quite generally, we note that with the condensation of a component, its corresponding normal gas component would have a lower density. For instance, the normal gas density of the $|+\rangle$ component is low in the trap center where the $|+\rangle$ condensed component resides. The middle column of Fig. 6 is the typical density distribution when $T \in (T_4, T_3]$. The condensed $|+\rangle$ component stays at the center and is surrounded by the $|0\rangle$ component. The condensed $|-\rangle$ component is too small to be visible directly, but can be perceived from the shallow well in its normal gas component, which indicates that the condensed $|-\rangle$ component is not zero and is lo-
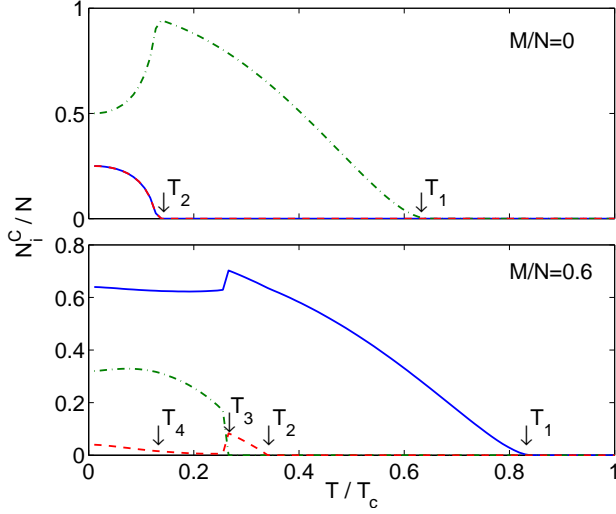
FIG. 7: The lowest excitation level for a gas of ^{87}Rb atoms at $M/N = 0.6$, $T/T_c = 0.34$ (right before the condensation of the $|-\rangle$ component). The inset shows the details of a zoomed-in plot near the minimum.

FIG. 5: Double condensations for ^{87}Rb atoms when $M = 0$ (the upper panel) and triple condensations for $M/N = 0.6$ (the lower panel). The solid line denotes the fractional population of the condensed $|+\rangle$ component, the dot-dashed line denotes the $|0\rangle$ component, and the dashed line denotes the $|-\rangle$ component.
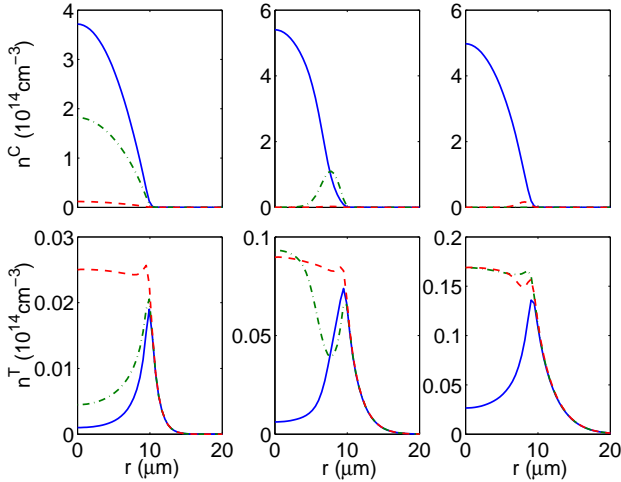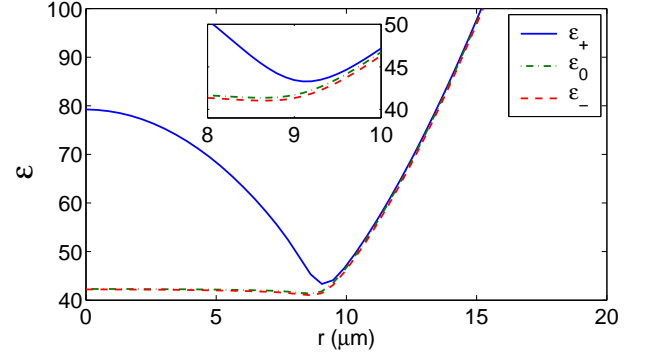

FIG. 6: Typical density distributions for a gas of ^{87}Rb atoms at $M/N = 0.6$. The left column is $T/T_c = 0.11$, the middle one is 0.21, and the right one 0.32. The notations are the same as in Fig. 3.

cated around the edge of the condensed $|+\rangle$ component. The left column of Fig. 6 shows the density distributions when $T \in (0, T_4]$, where all three condensed components coexist near the center of the trap and are surrounded by their normal gas components.

These results for ^{87}Rb atoms can be understood in terms of the interplay of three factors: ferromagnetic atom-atom interaction ($c_2 < 0$), the M conservation, and the miscibility between and among different components. The ferromagnetic interaction favors the most populated state, the M conservation sets an upper limit on the frac-

tion of the condensed $|+\rangle$ component, and the immiscibility between the condensed $|+\rangle$ and $|-\rangle$ component sets an upper limit on the total fraction of the condensed $|+\rangle$ and $|-\rangle$ components. For instance, in the region $T \in (T_2, T_1]$, only the $|+\rangle$ component condenses. The ferromagnetic interaction plays a dominant role and thus more atoms condense into the $|+\rangle$ state with decreasing temperature. In the region of $T \in (T_3, T_2]$, the M conservation and the immiscibility begin to take their effect. The M conservation causes the increases to the condensed $|+\rangle$ and $|-\rangle$ components to be almost identical, while the immiscibility makes the condensed $|-\rangle$ component stay outside the condensed $|+\rangle$ component. The system becomes unstable with the increase of the $|+\rangle$ and $|-\rangle$ components because with more condensed $|+\rangle$ component, the condensed $|-\rangle$ component must be pushed out further. Near the third critical temperature T_3, the condensed $|-\rangle$ component suddenly decreases to almost zero and the condensed $|+\rangle$ component decreases to about M. Approximately, the total decreased amount from the $|+\rangle$ and the $|-\rangle$ components becomes the condensed $|0\rangle$ component. The system enters the region $T \in (T_4, T_3]$ in which the condensed $|0\rangle$ component increases steadily with lowering temperature because the condensed $|+\rangle$ and $|0\rangle$ components are miscible. The condensed $|+\rangle$ component is almost independent of the temperature because of the M conservation. With decreasing temperatures, more and more condensed $|0\rangle$ component finally suppresses the immiscibility between $|+\rangle$ and $|-\rangle$ component at T_4, all three condensed components become miscible, and both the $|+\rangle$ and $|-\rangle$ components increase to keep M conserved while the $|0\rangle$ component decreases.

Figure 7 shows the lowest excitation energy $\varepsilon = \varepsilon(p = 0)$ for the three components of a ^{87}Rb gas at $M/N = 0.6$, $T/T_c = 0.34$ (right before the condensation of the $|-\rangle$ component). We see that the energy for the $|-\rangle$ component is lower than the corresponding ones for the other two states and takes a minimum near the spatial location of $r = 9$ μm, which is at the edge of the condensed $|+\rangle$ component. This result confirms that the $|-\rangle$ compo-

nent condenses before the $|0\rangle$ component and surrounds the condensed $|+\rangle$ component.

VI. CONCLUSION

We have studied the thermodynamics of Bose-Einstein condensation for a gas of spin-1 atoms with ferromagnetic and antiferromagnetic interactions using the mean field Hartree-Fock-Popov theory and the semiclassical approximation for the noncondensed components. Our results show that for antiferromagnetic interactions, double phase transitions persist as in a noninteracting gas: when $M > 0$, first the $|+\rangle$ component condenses, which is followed by the condensation of the $|-\rangle$ component on further decreasing of the temperature. The $|0\rangle$ component never condenses. For ferromagnetic interactions, on the other hand, our calculations reveal that the phase diagram becomes more complicated and a triple condensation scenario arises with decreasing temperatures: first the $|+\rangle$ component condenses, which is followed by the second condensation of the $|-\rangle$ component, and the third one for the $|0\rangle$ component. When the $|+\rangle$ and $|-\rangle$ components are the only condensed ones, they are immiscible. When all three components condense and the temperature is lower than T_4, they become miscible because of the presence of a large condensed $|0\rangle$ component. We have compared the numerically computed transition temperatures with that of an ideal gas as in Fig. 1. An overall lowering of the various transition temperatures due to atom-atom interactions is seen, consistent with the case of a single component interacting Bose gas, where the interaction-caused shift to the transition temperature has been actively studied [35]. Quite generally a repulsive interaction tends to lower the transition temperature for a single component Bose gas [24]. In the case of a spin-1 Bose gas considered here, $c_0 > 0$ and $c_0 \gg |c_2|$ constitutes an overall repulsive interaction.

Finally, we note there also exists the possibility of a ferromagnetic phase transition for ^{87}Rb atoms, in addition to the Bose-Einstein condensation as studied here. In fact, as was investigated recently by Gu and Klemm [36], the ferromagnetic transition is generally predicted to occur before, i.e. at temperatures higher than, the Bose Einstein condensation. The present study, however, remains unchanged because we treated the system within the global constraint of the conservation of total magnetization, distinct from that required for a separate ferromagnetic phase transition [36]. As is evidenced from recent experiments, the total magnetization M is well conserved, even better than the conservation of the total number N [11].

ACKNOWLEDGMENTS

[1] O. Mandel, M. Greiner, A. Widera, T. Rom, T. W. Hänsch, and I. Bloch, Nature (London) **425**, 937 (2004).

[2] C. A. Regal, M. Greiner, and D. S. Jin, Phys. Rev. Lett. **92**, 040403 (2004); M. W. Zwierlein *et al.*, *ibid* **92**, 120403 (2004).

[3] T. -L. Ho, Phys. Rev. Lett. **81**, 742 (1998).

[4] T. Ohmi and K. Machida, J. Phys. Soc. Jpn. **67**, 1822 (1998).

[5] C. K. Law, H. Pu, and N. P. Bigelow, Phys. Rev. Lett. **81**, 5257 (1998).

[6] M. V. Simkin and E. G. D. Cohen, Phys. Rev. A **59**, 1528 (1999).

[7] D. M. Stamper-Kurn, M. R. Andrews, A. P. Chikkatur, S. Inouye, H. -J. Miesner, J. Stenger, and W. Ketterle, Phys. Rev. Lett. **80**, 2027 (1998).

[8] A. Görlitz, T. L. Gustavson, A. E. Leanhardt, R. Löw, A. P. Chikkatur, S. Gupta, S. Inouye, D. E. Pritchard, and W. Ketterle, Phys. Rev. Lett. **90**, 090401 (2003).

[9] M. D. Barrett, J. A. Sauer, and M. S. Chapman, Phys. Rev. Lett. **87**, 010404 (2001).

[10] M. Erhard, H. Schmaljohann, J. Kronjäger, K. Bongs, and K. Sengstock, e-print cond-mat/0402003.

[11] M. -S. Chang, C. D. Hamley, M. D. Barrett, J. A. Sauer, K. M. Fortier, W. Zhang, L. You, and M. S. Chapman, Phys. Rev. Lett. **92**, 140403 (2004).

[12] H. Schmaljohann, M. Erhard, J. Kronjäger, M. Kottke, S. van Staa, L. Cacciapuoti, J. J. Arlt, K. Bongs, and K. Sengstock, Phys. Rev. Lett. **92**, 040402 (2004).

[13] H. -J. Miesner, D. M. Stamper-Kurn, J. Stenger, S. Inouye, A. P. Chikkatur, and W. Ketterle, Phys. Rev. Lett. **82**, 2228 (1999).

[14] D. M. Stamper-Kurn, H. -J. Miesner, A. P. Chikkatur, S. Inouye, J. Stenger, and W. Ketterle, Phys. Rev. Lett. **83**, 661 (1999).

[15] S. -K. Yip, Phys. Rev. Lett. **83**, 4677 (1999).

[16] T. Mizushima, K. Machida, and T. Kita, Phys. Rev. Lett. **89**, 030401 (2002).

[17] A. E. Leanhardt, Y. Shin, D. Kielpinski, D. E. Pritchard, and W. Ketterle, Phys. Rev. Lett. **90**, 140403 (2003).

[18] J. -P. Martikainen, A. Collin, and K. -A. Suominen, Phys. Rev. A **66**, 053604 (2002).

[19] T. Isoshima, T. Ohmi, and K. Machida, J. Phys. Soc. Jpn. **69**, 3864 (2000).

[20] W. -J. Huang, S. -C. Gou, and Y. -C. Tsai, Phys. Rev. A **65**, 063610 (2002).

[21] F. Gerbier, J. H. Thywissen, S. Richard, M. Hugbart, P. Bouyer, and A. Aspect, e-print cond-mat/0401585.

[22] V. Bagnato, D. E. Pritchard, and D. Kleppner, Phys. Rev. A **35**, 4354 (1987).

[23] W. Ketterle and N. J. van Druten, Phys. Rev. A **54**, 656 (1996).

[24] S. Giorgini, L. P. Pitaevskii, and S. Stringari, J. Low Temp. Phys. **109**, 309 (1997); Phys. Rev. A **54**, R4633 (1996).

[25] X. Liu, H. Hu, A. Minguzzi, and M. P. Tosi, e-print cond-mat/0311411 v1; A. Minguzzi, S. Conti, and M.

P. Tosi, J. Phys.: Condens. Matter **9**, L33 (1997).

[26] S. Yi, Ö. E. Müstecaplıoğlu, C. P. Sun, and L. You, Phys. Rev. A **66**, 011601 (2002).

[27] W. Zhang, S. Yi, and L. You, New J. Phys. **5**, 77 (2003).

[28] E. G. M. van Kempen, S. J. J. M. F. Kokkelmans, D. J. Heinzen, and B. J. Verhaar, Phys. Rev. Lett. **88**, 093201 (2002).

[29] A. Crubellier, O. Dulieu, F. Masnou-Seeuws, M. Elbs, H. Knöckel, and E. Tiemann, Eur. Phys. J. D **6**, 211 (1999).

[30] J. Stenger, S. Inouye, D. M. Stamper-Kurn, H. -J. Miesner, A. P. Chikkatur, and W. Ketterle, Nature (London) **396**, 345 (1998).

[31] D. M. Stamper-Kurn and W. Ketterle, in *Coherent Atomic Matter Waves*, Proceedings of the Les Houches Summer School in Theoretic Physics, Session LXXII, 1999, edited by R. Kaiser, C. Westbrook, and F. David (Springer, New York, 2001), pp. 137-217.

[32] T. -L. Ho, and S. K. Yip, Phys. Rev. Lett. **84**, 4031 (2000).

[33] M. Koashi and M. Ueda, Phys. Rev. Lett. **84**, 1066 (2000).

[34] A. J. Leggett, Rev. Mod. Phys. **73**, 307 (2001).

[35] M. Holzmann, G. Baym, J. Blaizot, and F. Laloë, Phys. Rev. Lett. **87**, 120403 (2001).

[36] Q. Gu and R. A. Klemm, Phys. Rev. A **68**, 031604(R) (2003).